The Market Price of Risk for Delivery Periods:

Pricing Swaps and Options in Electricity Markets*

ANNIKA KEMPER
annika.kemper@uni-bielefeld.de
Center for Mathematical Economics
Bielefeld University
PO Box 100131
33501 Bielefeld, Germany

MAREN D. SCHMECK
maren.schmeck@uni-bielefeld.de
Center for Mathematical Economics
Bielefeld University
PO Box 100131
33501 Bielefeld, Germany

ANNA KH. BALCI
akhripun@math.uni-bielefeld.de
Institute of Mathematics
Bielefeld University
PO Box 100131
33501 Bielefeld, Germany

22nd April 2020

Abstract

In electricity markets, futures contracts typically function as a swap since they deliver the underlying over a period of time. In this paper, we introduce a market price for the delivery periods of electricity swaps, thereby opening an arbitrage-free pricing framework for derivatives based on these contracts. Furthermore, we use a weighted *geometric averaging* of an artificial geometric futures price over the corresponding delivery period. Without any need for approximations, this averaging results in geometric swap price dynamics. Our framework allows for including typical features as the Samuelson effect, seasonalities, and stochastic volatility. In particular, we investigate the pricing procedures for electricity swaps and options in line with Arismendi et al. (2016), Schneider and Tavin (2018), and Fanelli and Schmeck (2019). A numerical study highlights the differences between these models depending on the delivery period.

JEL CLASSIFICATION: G130 · Q400

KEYWORDS: Electricity Swaps · Delivery Period · Market Price of Delivery Risk · Seasonality · Samuelson Effect · Stochastic Volatility · Option Pricing · Heston model

*Financial support by the German Research Foundation (DFG) through the Collaborative Research Centre 'Taming uncertainty and profiting from randomness and low regularity in analysis, stochastics and their applications' is gratefully acknowledged.

1. Introduction

Futures contracts are the most important derivatives in electricity- and commodity markets. Due to the non-storability of electricity, the underlying is typically delivered over a period, and the contract is therefore referred to as a swap. In electricity markets, the delivery period has an influence on price dynamics, and Fanelli and Schmeck (2019) have provided empirical evidence indicating that implied volatilities of electricity options are seasonal with respect to the delivery period. In other words, the distributional features – or the pricing measure – depend on the delivery period of the contract. In this paper, we introduce an arbitrage-free pricing framework that takes dependencies on the delivery into account. The core of our approach is the so-called *market price of delivery risk*, which reflects expectations about variations in volatility weighted over the delivery period and arises through a *geometric average* approach similar to that used by Kemna and Vorst (1990).

In fact, the delivery period is one of the features that distinguishes electricity markets from other commodity markets such as oil, gas, or corn. An easy way to acknowledge its existence is to use futures price dynamics with a delivery time that represents the midpoint of the delivery period. This approach has been followed, for example, by Schmeck (2016), and is advantageous as it captures the typically observed behavior that the futures prices do not converge against the electricity spot price if time approaches the beginning of the delivery. A possible way to model the delivery period explicitly is to average the spot price or an artificial futures price over the entire delivery time. Typically, *arithmetic averaging* is used, which is the standard approach in electricity price modeling and works especially well for arithmetic price dynamics (see, e.g., Benth et al. (2008), and Benth et al. (2019)). However, if the underlying electricity futures are of the geometric type, the resulting dynamics are neither geometric nor Markovian. In that case, the dynamics are approximated in line with Bjerksund et al. (2010) (see also Benth et al. (2008)).

A typical feature of electricity markets is the seasonal behavior of prices. The effect is enforced through the rise of renewable energy, which is highly dependent on weather conditions. At present, there is a growing worldwide trend to acknowledge the need for sustainable energy production, which also raises the expectations of a further increasing impact of seasonal effect. Among others, Arismendi et al. (2016), Borovkova and Schmeck (2017), and Fanelli and Schmeck (2019) have addressed and modeled seasonality in either commodity- or energy markets. Typically, a deterministic seasonal price level is added to the price dynamics, but the dynamics can also exhibit seasonal behavior. Fanelli and Schmeck (2019) distinguish between *seasonalities in the trading day* and *seasonalities in the delivery period*. Arismendi et al. (2016) suggest the use of a seasonal stochastic volatility model for commodity futures. As in the Heston model, stochastic volatility follows a square-root process, but with a seasonal mean-reversion level. Indeed, a volatility smile can also be observed in electricity option markets (see Figure 1) such that a stochastic volatility model seems appropriate.

Finally, a well-known feature in electricity- and commodity markets is the Samuelson effect (see

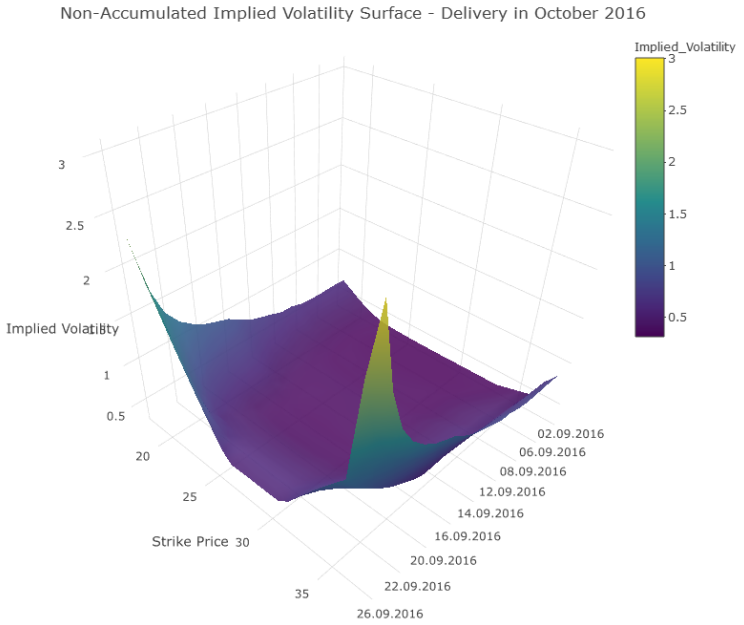

Figure 1 *The implied non-accumulated volatility surface with respect to strikes from 18 to 38 over the last trading month in September 2016 for a European option on the Phelix DE/AU Baseload Month futures at the European Energy Exchange (EEX) delivering in October 2016.*

Samuelson (1965)), which implies that futures close to delivery are much more volatile than are those whose expiration date lies far off. This effect can be observed in the implied volatility of electricity options, especially far out and in the money (see also Figure 1 and Kiesel et al. (2009)). The effect is typically included in any electricity futures price dynamics. Schneider and Tavin (2018) include such a term-structure effect within the framework of stochastic volatility modeling. Schmeck (2016) investigates analytically the impact of the Samuelson effect on option pricing.

In this paper, we suggest modeling the delivery period explicitly through a *geometric averaging* approach for electricity futures prices of the geometric type, in line with Kemna and Vorst (1990) and Bjerksund et al. (2010). This approach leads directly to Markovian and geometric swap price dynamics. Indeed, the geometric averaging of futures prices coincides with the arithmetic procedure applied to logarithmic futures prices. In line with the literature, we base the averaging procedure on an artificial futures contract that is a martingale under a pricing measure $\mathbb{Q}$. In our framework, the resulting swap price dynamics are not a martingale under $\mathbb{Q}$ due to a drift term in the dynamics that is characterized by the variance of the weighted delivery and is used to define the market price of delivery risk and an equivalent martingale measure $\widetilde{\mathbb{Q}}$ for the swap price. $\widetilde{\mathbb{Q}}$ can thus be used as a pricing measure for derivatives on the swap. We characterize the market price of delivery risk for the Samuelson effect, and for seasonalities in the trading day and in the delivery period following Schneider and Tavin (2018), Arismendi et al. (2016), and Fanelli and Schmeck (2019), respectively.

For option pricing, we consider a general stochastic volatility model that is inter alia feasible for mean-reverting square-root volatility processes in line with the models used by Arismendi et al. (2016) and Schneider and Tavin (2018). The volatility structure is rich enough to include the categories of seasonalities and the Samuelson effect. Both models share the feature that their commodity futures prices are based on an affine stochastic volatility structure. Indeed, the averaging procedure of the futures price model as well as the change of measure preserve the affine model structure of the artificial futures price dynamics.
In this paper, we focus on the pricing of a single swap contract. As mentioned above, the pricing measure depends on this particular contract, and it thus cannot be used for pricing derivatives on another swap contract with a different delivery period. Nevertheless, several swap contracts are usually also tradable, such that arbitrage possibilities must be excluded. Furthermore, overlapping delivery periods are tradable as a quarter and the corresponding three months. We address how to tackle these issues in Chapter 4.

The paper is organized as follows: Chapter 2 presents the geometric averaging approach and introduces the market price of delivery based on a general stochastic volatility model. In order to illustrate the averaging procedure, we discuss the method based on the models created by Arismendi et al. (2016), Schneider and Tavin (2018), and Fanelli and Schmeck (2019) in Chapter 3. In Chapter 4, we address how to exclude arbitrage opportunities that might appear when there are several, possibly overlapping swap contracts traded on the market. Option pricing is discussed in Chapter 5. In addition, all adjusted commodity market models are investigated numerically. Finally, Chapter 6 presents our conclusions.

2. Averaging of Futures Contracts

We consider a swap contract delivering a flow of 1 Mwh electricity during the delivery period $(\tau_1, \tau_2]$. At a trading day $t \leq \tau_1$, the swap price is denoted by $F(t, \tau_1, \tau_2)$ and settled such that the contract is entered at no cost. It can be interpreted as an average price of instantaneous delivery. Motivated by this interpretation, we consider an artificial futures contract with price $F(t, \tau)$ that stands for instantaneous delivery at time $\tau \in (\tau_1, \tau_2]$. Note that such a contract does not exist on the market, but turns out to be useful for modeling purposes when considering delivery periods (see for example Benth et al. (2019)).

Consider a filtered probability space $(\Omega, \mathcal{F}, (\mathcal{F}_t)_{t\in[0,\tau]}, \mathbb{Q})$, where the filtration satisfies the usual conditions. At time $t \leq \tau$, the price of the futures contract follows a geometric diffusion process

evolving as

$$dF(t,\tau) = \sigma(t,\tau)F(t,\tau)dW^F(t) \ , \tag{2.1}$$

$$d\sigma^2(t,\tau) = a(t,\tau,\sigma)dt + c(t,\tau,\sigma)dW^\sigma(t) \ , \tag{2.2}$$

with initial conditions $F(0,\tau) = F_0 > 0$ and $\sigma^2(0,\tau) = \sigma_0^2 > 0$, and where W^F and W^σ are correlated standard Brownian motions under $\mathbb{Q}$. Thus, $W^\sigma = \rho W^F + \sqrt{1-\rho^2}W$ for a Brownian motion W independent of W^F and $\rho \in (-1,1)$. We assume that both, the futures price volatility $\sigma(t,\tau)$ and the futures price $F(t,\tau)$, are $\mathcal{F}_t$-adapted for $t \in [0,\tau]$, and that they satisfy suitable integrability and measurability conditions to ensure that (2.1) is a $\mathbb{Q}$-martingale, and the solution given by

$$F(t,\tau) = F(0,\tau)e^{\int_0^t \sigma(s,\tau)dW^F(s) - \frac{1}{2}\int_0^t \sigma^2(s,\tau)ds} \tag{2.3}$$

exists (see Appendix A for details). As $\sigma(t,\tau)$ depends on both time t and delivery time τ, we allow for volatility structures as the Samuelson effect, seasonalities in the trading day, or seasonalities in the delivery time. In this framework, we would like to mention the models of Arismendi et al. (2016), Schneider and Tavin (2018), as well as of Fanelli and Schmeck (2019), which are addressed in the next chapter.

Following the Heath-Jarrow-Morton approach to price futures and swaps in electricity markets, the swap price is usually defined as the *arithmetic average* of futures prices (see, e.g., Benth et al. (2008), Bjerksund et al. (2010), and Benth et al. (2019)):

$$F^a(t,\tau_1,\tau_2) = \int_{\tau_1}^{\tau_2} w(u,\tau_1,\tau_2)F(t,u)du \ , \tag{2.4}$$

for a general weight function

$$w(u,\tau_1,\tau_2) := \frac{\hat{w}(u)}{\int_{\tau_1}^{\tau_2}\hat{w}(v)dv} \ , \quad \text{for } u \in (\tau_1,\tau_2] \ . \tag{2.5}$$

The most popular example is given by $\hat{w}(u) = 1$, such that $w(u,\tau_1,\tau_2) = \frac{1}{\tau_2-\tau_1}$. This corresponds to a one-time settlement. A continuous settlement over the time interval $(\tau_1,\tau_2]$ is covered by $\hat{w}(u) = e^{-ru}$, where $r \geq 0$ is the constant interest rate (see, e.g., Benth et al. (2008)). The arithmetic average of the futures price as in (2.4) leads to tractable dynamics for the swap as long as one assumes an arithmetic structure of the futures prices as well. This is based on the fact that arithmetic averaging is tailor-made for absolute growth rate models. Nevertheless, if one defines the futures price as a geometric process as in (2.1), one can show that the dynamics of the swap defined through (2.4) is given by

$$dF^a(t,\tau_1,\tau_2) = \sigma(t,\tau_2)F^a(t,\tau_1,\tau_2)dW^F(t) - \int_{\tau_1}^{\tau_2}\frac{\partial\sigma}{\partial u}(t,u)\frac{w(\tau,\tau_1,\tau_2)}{w(\tau,\tau_1,u)}F^a(t,\tau_1,u)du\ dW^F(t) \ ,$$

for any $\tau \in (\tau_1, \tau_2]$ (see Benth et al. (2008); Chapter 6.3.1). Thus, the dynamics of the swap price is neither a geometric process nor Markovian, which makes it unhandy for further analysis. Bjerksund et al. (2010) suggest an approximation given by

$$dF^a(t,\tau_1,\tau_2) = F^a(t,\tau_1,\tau_2)\Sigma(t,\tau_1,\tau_2)dW^F(t) \ , \tag{2.6}$$

where $F^a(0,\tau_1,\tau_2) = F_0$ and an weighted average volatility

$$\Sigma(t,\tau_1,\tau_2) := \int_{\tau_1}^{\tau_2} w(u,\tau_1,\tau_2)\sigma(t,u)du \ . \tag{2.7}$$

Instead of averaging absolut price trends as in (2.4), we here suggest to focus on the averaging procedure of relative price trends, i.e. growth rates or logarithmic prices. This leads to a *geometric averaging* procedure in continuous time. In fact, the connection between exponential models and geometric averaging seems natural: the geometric averaging of a geometric price process corresponds to an arithmetic average of logarithmic prices. Note that this approach is in line with Kemna and Vorst (1990) for pricing average asset value options on equities and also with Bjerksund et al. (2010). The difference of Bjerksund et al. (2010) and our approach is, that Bjerksund et al. (2010) approximate the geometric average to receive a martingale dynamics, while we will make a change of measure. Note that the choice of pricing measures in electricity markets allows for more freedom as in other markets, as electricity itself is not storable, and thus no-arbitrage considerations for the spot itself are not applicable (see Benth and Schmeck (2014)).

We define the swap price as

$$F(t,\tau_1,\tau_2) := \exp\left(\int_{\tau_1}^{\tau_2} w(u,\tau_1,\tau_2)\log(F(t,u))du\right) \ . \tag{2.8}$$

Assume that the volatility satisfies further integrability conditions (see Appendix A). It turns out, that the resulting swap price dynamics is a geometric process with stochastic swap price volatility $\Sigma(t,\tau_1,\tau_2)$:

Lemma 1. *The dynamics of the swap price defined in* (2.8) *under* $\mathbb{Q}$ *is given by*

$$\frac{dF(t,\tau_1,\tau_2)}{F(t,\tau_1,\tau_2)} = \frac{1}{2}\left(\Sigma^2(t,\tau_1,\tau_2) - \int_{\tau_1}^{\tau_2} w(u,\tau_1,\tau_2)\sigma^2(t,u)du\right)dt + \Sigma(t,\tau_1,\tau_2)\ dW^F(t) \ . \tag{2.9}$$

Proof. Plugging (2.3) into (2.8) and using the stochastic Fubini Theorem (see Protter (2005); Theorem 65) leads to

$$F(t,\tau_1,\tau_2) = F(0,\tau_1,\tau_2)e^{-\frac{1}{2}\int_0^t\int_{\tau_1}^{\tau_2} w(u,\tau_1,\tau_2)\sigma^2(s,u)du\ ds + \int_0^t \Sigma(s,\tau_1,\tau_2)\ dW^F(s)} \ . \tag{2.10}$$

Then, (2.9) follows using Itô's formula. □

Although the futures price $F(t,\tau)$ is a martingale under the pricing measure $\mathbb{Q}$, the swap price $F(t,\tau_1,\tau_2)$ is not a $\mathbb{Q}$-martingale anymore: the swap price under $\mathbb{Q}$ has a drift term, given by the difference between the swap price's variance and the weighted average of the futures price variance. We thus define a *market price of risk* at time $t \in [0,\tau_1]$ associated to the delivery period $(\tau_1,\tau_2]$ as

$$b_1(t,\tau_1,\tau_2) := \frac{1}{2}\frac{\int_{\tau_1}^{\tau_2} w(u,\tau_1,\tau_2)\sigma^2(t,u)du - \Sigma^2(t,\tau_1,\tau_2)}{\Sigma(t,\tau_1,\tau_2)} \,, \tag{2.11}$$

where $b_1(t,\tau_1,\tau_2)$ is measurable and $\mathcal{F}_t$-adapted as $\sigma(t,u)$ and $\Sigma(t,\tau_1,\tau_2)$ are. It can be interpreted as the trade-off between the weighted average variance of a stream of futures on the one hand and the variance of the swap on the other hand. Since we have two independent Brownian motions, W^F and W, we have a two-dimensional market price of risk $b(t,\tau_1,\tau_2) = (b_1(t,\tau_1,\tau_2), b_2)^\intercal$, where we choose $b_2 = 0$. The market price $b_1(\cdot,\tau_1,\tau_2)$ will enter also the dynamics of the volatility, which is driven by the Brownian motion $W^\sigma = \rho W^F + \sqrt{1-\rho^2}W$.

Remark 1. *For a random variable U with density $w(u,\tau_1,\tau_2)$, we can write*

$$\begin{aligned}\Sigma(t,\tau_1,\tau_2) &= \mathbb{E}_U[\sigma(t,U)] \,,\\ b_1(t,\tau_1,\tau_2) &= \frac{1}{2}\frac{\mathbb{V}_U[\sigma(t,U)]}{\mathbb{E}_U[\sigma(t,U)]} \,,\end{aligned}$$

where $\mathbb{E}_U$ and $\mathbb{V}_U$ denote the expectation and variance only with respect to the random variable U. Note that $\sigma(t,U)$ identifies the futures price volatility for a random time of delivery. Hence, the market price of delivery risk is the variance per unit of expectation of $\sigma(t,U)$. This is very similar to the well-known coefficient of variation $\frac{\sqrt{\mathbb{V}_U[\sigma(t,U)]}}{\mathbb{E}_U[\sigma(t,U)]}$.

We define a new pricing measure $\widetilde{\mathbb{Q}}$, such that $F(\cdot,\tau_1,\tau_2)$ is a martingale. Define the Radon-Nikodym density through

$$Z(t,\tau_1,\tau_2) := \exp\left\{-\int_0^t b_1(s,\tau_1,\tau_2)dW^F(s) - \frac{1}{2}\int_0^t b_1^2(s,\tau_1,\tau_2)ds\right\} \,.$$

Assume that

$$\mathbb{E}_{\mathbb{Q}}\left[Z(\tau_1,\tau_1,\tau_2)\right] = 1 \,, \tag{2.12}$$

which means $Z(\cdot,\tau_1,\tau_2)$ is indeed a martingale for the entire trading time. We will show later that Novikov's condition (see, e.g., Karatzas and Shreve (1991)) is fullfilled for suitable models, such that (2.12) holds true. We then define the new measure $\widetilde{\mathbb{Q}}$ through the Radon Nikodym density

$$\frac{d\widetilde{\mathbb{Q}}}{d\mathbb{Q}} := Z(\tau_1,\tau_1,\tau_2) \,,$$

which clearly depends on the delivery period $(\tau_1, \tau_2]$. Girsanov's theorem states that

$$\widetilde{W}^F(t) = W^F(t) + \int_0^t b_1(s, \tau_1, \tau_2) ds \ , \tag{2.13}$$

$$\widetilde{W}(t) = W(t) \ , \tag{2.14}$$

are standard Brownian motions under $\widetilde{\mathbb{Q}}$ (see, e.g., Shreve (2004)). The Brownian motion of the stochastic volatility is also affected due to the correlation structure:

$$\widetilde{W}^\sigma(t) = W^\sigma(t) + \int_0^t \rho b_1(s, \tau_1, \tau_2) ds \ . \tag{2.15}$$

A straight forward valuation leads to the following result:

Proposition 1. *The swap price* $F(t, \tau_1, \tau_2)$ *defined in* (2.8) *is a martingale under* $\widetilde{\mathbb{Q}}$*. The swap price and volatility dynamics are given by*

$$\frac{dF(t, \tau_1, \tau_2)}{F(t, \tau_1, \tau_2)} = \Sigma(t, \tau_1, \tau_2) \, d\widetilde{W}^F(t) \ , \tag{2.16}$$

$$d\sigma^2(t, \tau) = \left(a(t, \tau, \sigma) - \rho b_1(t, \tau_1, \tau_2) c(t, \tau, \sigma)\right) dt + c(t, \tau, \sigma) d\widetilde{W}^\sigma(t) \ , \tag{2.17}$$

where $\Sigma(t, \tau_1, \tau_2)$ *is defined in* (2.7)*.*

Note that the stochastic volatility process $\sigma^2(t, \tau)$ also depends on the delivery interval, which we drop for notational convenience. As the swap price $F(t, \tau_1, \tau_2)$ is a martingale under the equivalent measure $\widetilde{\mathbb{Q}}$, we can use it to price options on the swap. Nevertheless, $\widetilde{\mathbb{Q}}$ depends on the particular delivery period of the swap and cannot be used to price options on swaps on other delivery periods. We address this issue in Chapter 4.1.

We would like to compare the approximated swap price $F^a(t, \tau_1, \tau_2)$ under $\mathbb{Q}$ following Bjerksund et al. (2010) with the swap price $F(t, \tau_1, \tau_2)$ under $\widetilde{\mathbb{Q}}$ as defined in (2.8) assuming that both have a stochastic volatility based on (2.2). The swap price dynamics have the same form, the difference is in the drift term of the stochastic volatility. If the volatility is deterministic as in the setting of Bjerksund et al. (2010), the distribution of $F^a(t, \tau_1, \tau_2)$ under $\mathbb{Q}$ and the distribution of $F(t, \tau_1, \tau_2)$ under $\widetilde{\mathbb{Q}}$ are the same. For the swap prices both under the same measure we have the following result.

Lemma 2. *For the swap prices* $F^a(t, \tau_1, \tau_2)$ *and* $F(t, \tau_1, \tau_2)$*, both under* $\mathbb{Q}$*, it holds that*

$$F(t, \tau_1, \tau_2) - F^a(t, \tau_1, \tau_2) = F^a(t, \tau_1, \tau_2) \left[e^{\frac{1}{2} \int_0^t \mathbb{V}_U[\sigma(s,U)] ds} - 1 \right] \geq 0 \ .$$

Proof. From (2.6), we know that

$$F^a(t, \tau_1, \tau_2) = F_0 e^{-\frac{1}{2} \int_0^t \Sigma^2(s, \tau_1, \tau_2) ds + \int_0^t \Sigma(s, \tau_1, \tau_2) dW^F(s)} \ .$$

Using equation (2.10) and the notation from Remark 1, we find

$$F^a(t,\tau_1,\tau_2) = F(t,\tau_1,\tau_2)e^{-\frac{1}{2}\int_0^t \mathbb{V}_U[\sigma(s,U)]ds} \tag{2.18}$$

and the result follows. The expression in squared brackets is strictly positive as it is the case for the variance. □

Note that in (2.18) $\mathbb{V}_U\left[\sigma(s,U)\right]$ can be interpreted as discount rate.

3. Electricity Swap Price Models

In this chapter, we transform three commodity market models from the recent literature into electricity swap models using the geometric averaging procedure presented in Chapter 2. That is, we examine the influence of seasonality in the mean-reversion level of the (stochastic) volatility following Arismendi et al. (2016), the impact of the Samuelson effect in line with Schneider and Tavin (2018), as well as the seasonal dependence on the delivery time following Fanelli and Schmeck (2019). Moreover, we investigate the corresponding swap and market prices numerically. In Chapter 5, we then adress option pricing for these three models.

3.1. Seasonal Dependence on the Trading Day

Arismendi et al. (2016) consider a generalized Heston model, where the mean-reversion rate of the stochastic volatility is seasonal. That is, they suggest a futures price dynamics of the form

$$dF(t,\tau) = \sqrt{\nu(t)}F(t,\tau)dW^F(t)\ , \tag{3.1}$$

$$d\nu(t) = \kappa\left(\theta(t)-\nu(t)\right)dt + \sigma\sqrt{\nu(t)}dW^\sigma(t)\ , \tag{3.2}$$

where W^σ and W^F are defined as before under $\mathbb{Q}$. The stochastic volatility $\nu(t)$ is given by a Cox-Ingersoll-Ross process with a time-dependent level. The Feller condition $2\kappa\theta^{\min} > \sigma^2$ needs to be satisfied with $\theta^{\min} := \min_{t\in[0,\tau]}\theta(t)$ in order to receive a strictly positive solution. If the mean-reversion level $\theta(t)$ is in particular of exponential sinusoidal form, that is $\theta(t) = \alpha e^{\beta\sin(2\pi(t+\gamma))}$, for $\alpha,\beta>0,\gamma\in[0,1)$, then $\theta^{\min} = \alpha e^{-\beta}$. In the framework of Chapter 2, the futures price volatility is given by $\sigma(t,\tau) = \sqrt{\nu(t)}$. The corresponding swap price dynamics under the $\mathbb{Q}$ evolve as

$$dF(t,\tau_1,\tau_2) = \sqrt{\nu(t)}F(t,\tau_1,\tau_2)dW^F(t)\ , \tag{3.3}$$

$$d\nu(t) = \kappa(\theta(t)-\nu(t))dt + \sigma\sqrt{\nu(t)}dW^\sigma(t)\ . \tag{3.4}$$

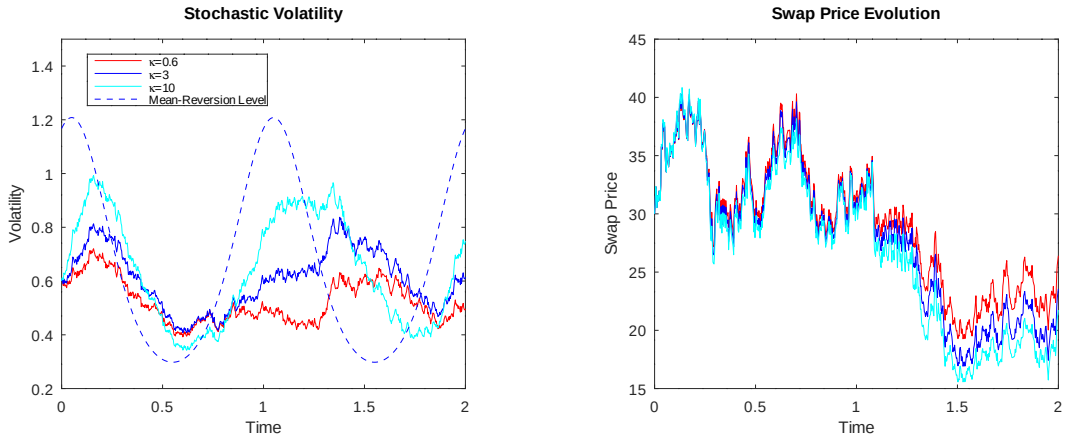

Figure 2 *Stochastic volatility for different choices of mean-reversion speed and the corresponding mean-reversion level (left). Swap prices based on the stochastic volatilities (right). For the choice of parameters, see Table 2 in Chapter 3.4.*

Typical trajectories of the volatility and swap prices are illustrated in Figure 2. As the futures price volatility does not depend on the delivery time τ, the resulting volatility of the swap is given by the futures price volatility

$$\Sigma(t, \tau_1, \tau_2) = \sqrt{\nu(t)} \, , \tag{3.5}$$

for all choices of weight functions $w(\cdot, \tau_1, \tau_2)$. Then, the market price of the delivery period is also zero, that is

$$b_1(t, \tau_1, \tau_2) = 0 \, , \tag{3.6}$$

for all $t \in [0, \tau_1]$ and we arrive directly at swap price dynamics of martingale form. Since the model is not linked to the delivery time, the pricing measures for the futures and swap contract coincide, as the dynamics do. In Figure 2, we illustate the model for different speed of mean-reversion parameters of the volatility process. The higher the parameter κ, the closer the seasonal mean-reversion level is reached by the stochastic volatility, and the higher the stochastic volatility oscillates. This affects the swap price evolution as well.

3.2. Samuelson Effect

Schneider and Tavin (2018) include the so-called Samuelson effect within the framework of a futures price model under stochastic volatility. The Samuelson effect describes the empirical observation that the variations of futures increase the closer the expiration date is reached (see also Samuelson (1965)). Typically this is captured with an exponential alteration in the volatility of the form $e^{-\lambda(\tau - t)}$, for $\lambda > 0$. For $t \to \tau$, the term converges to 1 and the full volatility enters the dynamics.

If the time to maturity increases, that is for $\tau - t \to \infty$, the volatility decreases. While Schneider and Tavin (2018) base their model on a multi-dimensional setting, we here focus on the one-dimensional case following

$$dF(t,\tau) = e^{-\lambda(\tau-t)}\sqrt{\nu(t)}F(t,\tau)dW^F(t)\ , \tag{3.7}$$

$$d\nu(t) = \kappa(\theta - \nu(t))dt + \sigma\sqrt{\nu(t)}dW^\sigma(t)\ . \tag{3.8}$$

This approach includes a term-structure in the volatiliy process of the form $\sigma(t,\tau) = e^{-\lambda(\tau-t)}\sqrt{\nu(t)}$. Applying the geometric averaging method as in (2.8) with weight function $\hat{w}(u) = 1$, the volatility of the swap is

$$\Sigma(t,\tau_1,\tau_2) = d_1(\tau_2 - \tau_1)e^{-\lambda(\tau_1-t)}\sqrt{\nu(t)}\ , \tag{3.9}$$

and the new swap martingale measure $\widetilde{\mathbb{Q}}$ is defined via the market price of risk

$$b_1(t,\tau_1,\tau_2) = d_2(\tau_2 - \tau_1)e^{-\lambda(\tau_1-t)}\sqrt{\nu(t)}\ , \tag{3.10}$$

where

$$d_1(x) = \frac{1-e^{-\lambda x}}{\lambda x} \quad \text{and} \quad d_2(x) = \frac{1}{2}\left(\frac{1}{2}(1+e^{-\lambda x}) - d_1(x)\right)\ . \tag{3.11}$$

The volatility and the market price of risk factorize into three parts: a constant $d_2(\tau_2 - \tau_1)$ depending only on the length of the delivery period, the Samuelson effect counting the time to maturity at τ_1, and the stochastic volatility $\sqrt{\nu(t)}$. The Samuelson effect enters both swap price dynamics and market price of risk through the term $e^{-\lambda(\tau_1-t)}$. Σ and b_1 become small if we are far away from maturity, and increases exponentially if we approach the maturity of the option. The swap price dynamics under $\widetilde{\mathbb{Q}}$ are given by

$$dF(t,\tau_1,\tau_2) = \Sigma(t,\tau_1,\tau_2)F(t,\tau_1,\tau_2)d\widetilde{W}^F(t)\ , \tag{3.12}$$

$$d\nu(t) = \left(\kappa\theta - \left[\kappa + \rho\sigma d_2(\tau_2-\tau_1)e^{-\lambda(\tau_1-t)}\right]\nu(t)\right)dt + \sigma\sqrt{\nu(t)}d\widetilde{W}^\sigma(t)\ . \tag{3.13}$$

We observe that the drift of the dynamics of $\nu(t)$ is now altered by the market price of risk, which again depends on the delivery period. The speed of mean reversion is now given by

$$\kappa + \rho\sigma d_2(\tau_2-\tau_1)e^{-\lambda(\tau_1-t)} \begin{cases} \geq \kappa\ , & \text{if} \quad \rho \geq 0\ , \\ < \kappa\ , & \text{if} \quad \rho < 0\ . \end{cases}$$

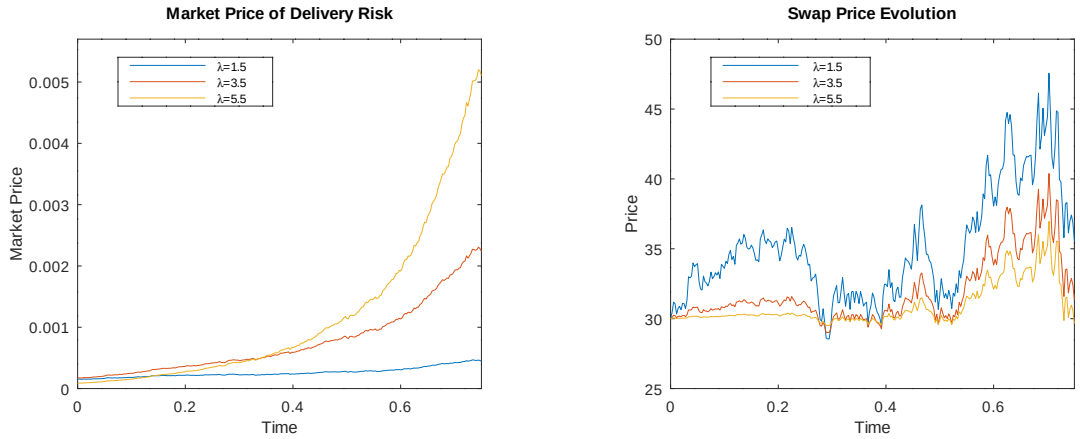

Figure 3 *Market prices of delivery risk (left) and swap prices under $\widetilde{\mathbb{Q}}$ (right) both for different values for λ.*

The mean reversion level is given by

$$\frac{\kappa}{\kappa + \rho\sigma d_2(\tau_2 - \tau_1)e^{-\lambda(\tau_1 - t)}}\theta \begin{cases} \leq \theta\,, & \text{if} \quad \rho \geq 0\,, \\ > \theta\,, & \text{if} \quad \rho < 0\,. \end{cases}$$

For a positive correlation between swap price- and volatility dynamcis, the speed of mean reversion increases and the level of mean reversion decreases and vice versa for a negative correlation. If $8\kappa^2 > \sigma^2 \max\{1; \frac{1}{\lambda^2(\tau_2-\tau_1)^2}\}$, Novikov's condition is satisfied such that the measure change is well defined and $F(t, \tau_1, \tau_2)$ is indeed a true martingale under $\widetilde{\mathbb{Q}}$ (see Appendix B). Using the notation of Remark 1, we can write

$$\begin{aligned} \Sigma(t, \tau_1, \tau_2) &= \mathbb{E}[e^{-\lambda(U-\tau_1)}]e^{-\lambda(\tau_1 - t)}\sqrt{\nu(t)}\,, \\ b_1(t, \tau_1, \tau_2) &= \frac{1}{2}\frac{\mathbb{V}[e^{-\lambda(U-\tau_1)}]}{\mathbb{E}[e^{-\lambda(U-\tau_1)}]}e^{-\lambda(\tau_1 - t)}\sqrt{\nu(t)}\,, \end{aligned}$$

for a random variable $U \sim \mathcal{U}[\tau_1, \tau_2]$. The impact of the Samuelson effect on the market price of risk as well as the swap price dynamics is illustrated in Figure 3. The parameters are chosen as in Table 2 (see Chapter 5.2.4).The exponential behavior of the market price becomes more pronounced the higher the Samuelson parameter λ. At terminal time, it is equal to $d_2(\frac{1}{12})$, which depends by definition on λ (see Equation (3.11) and Table 1). Moreover, we clearly observe the Samuelson effect within the swap price evolution. The higher the Samuelson parameter, the smaller the variance of the Samuelson effect (see Table 1), and thus the smaller the swap's variance (see Figure 3). However, the closer we reach the expiration date, the higher the swap price volatility.

Table 1 *Expectation, variance and market price of delivery risk for different Samuelson parameters.*

	$d_1(\frac{1}{12}) = \mathbb{E}\left[e^{-\lambda(U-\tau_1)}\right]$	$\mathbb{V}\left[e^{-\lambda(U-\tau_1)}\right]$	$d_2(\frac{1}{12})$
$\lambda = 1.5$	0.9400	0.0012	0.0006
$\lambda = 3.5$	0.8674	0.0053	0.0031
$\lambda = 5.5$	0.8022	0.0112	0.0070

3.3. Delivery-Dependent Seasonality

Fanelli and Schmeck (2019) show that the implied volatilities of electricity options depend on the delivery period in a seasonal fashion. Incorporating this idea into a stochastic volatility framework, we start with the following futures price dynamics under $\mathbb{Q}$:

$$dF(t,\tau) = s(\tau)\sqrt{\nu(t)}F(t,\tau)dW^F(t)\ , \tag{3.14}$$

$$dv(t) = \kappa(\theta - \nu(t))dt + \sigma\sqrt{\nu(t)}dW^\sigma(t)\ . \tag{3.15}$$

Here, $s(\tau)$ models the seasonal dependence on the delivery in τ. Deriving the swap price model as in Chapter 2, again with the choice of $\hat{w}(u) = 1$, the swap price volatility is given by

$$\Sigma(t,\tau_1,\tau_2) = S_1(\tau_1,\tau_2)\sqrt{\nu(t)}\ . \tag{3.16}$$

Moreover, the swap's pricing measure $\widetilde{\mathbb{Q}}$ is defined via the market price of risk

$$b_1(t,\tau_1,\tau_2) = S_2(\tau_1,\tau_2)\sqrt{\nu(t)}\ , \tag{3.17}$$

where

$$S_1(\tau_1,\tau_2) = \frac{1}{\tau_2-\tau_1}\int_{\tau_1}^{\tau_2} s(u)du \tag{3.18}$$

and

$$S_2(\tau_1,\tau_2) = \frac{1}{2}\left(\frac{\frac{1}{\tau_2-\tau_1}\int_{\tau_1}^{\tau_2} s^2(u)du - S_1(\tau_1,\tau_2)^2}{S_1(\tau_1,\tau_2)}\right)\ . \tag{3.19}$$

Here, $S_1(\tau_1,\tau_2)$ describes the average seasonality in the volatility during the delivery period, and $S_2(\tau_1,\tau_2)$ the relative trade-off between the average squared seasonaltity (resulting from the average variance of a stream of futures) and the squared average seasonality (e.g. the variance part of the

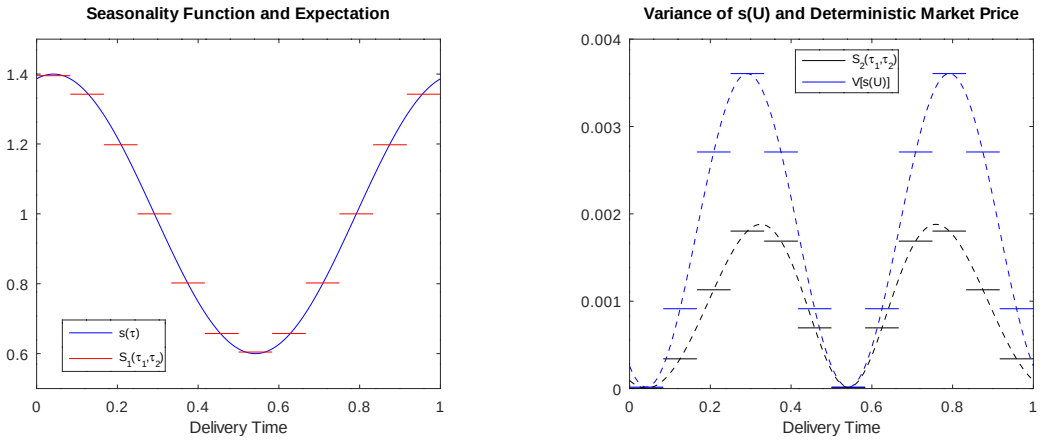

Figure 4 *$s(\tau)$ and $S_1(\tau_1, \tau_2)$ for different delivery periods over one year (left). $S_2(\tau_1, \tau_2)$ and the variance of $s(\tau)$ with respect to the delivery time (right).*

average seasonality). The swap price dynamics under $\widetilde{\mathbb{Q}}$ then follow

$$dF(t, \tau_1, \tau_2) = S_1(\tau_1, \tau_2)\sqrt{\nu(t)}F(t, \tau_1, \tau_2)d\widetilde{W}^F(t) \,, \tag{3.20}$$

$$d\nu(t) = (\kappa\theta - [\kappa + \sigma\rho S_2(\tau_1, \tau_2)]\nu(t)) + \sigma\sqrt{\nu(t)}d\widetilde{W}^\sigma(t) \,. \tag{3.21}$$

A possible choice for the seasonality function is $s(\tau) = a + b\cos(2\pi(\tau + c))$, where $a > b > 0$ and $c \in [0, 1)$ to ensure that the volatility stays positive. In this case, Novikov's condition is satisfied if $\kappa^2 > \alpha^2\sigma^2$, such that the measure change is well defined and F is indeed a true martingale under $\widetilde{\mathbb{Q}}$ (see Appendix B). In the setting of Remark 1, we have

$$\Sigma(t, \tau_1, \tau_2) = \mathbb{E}[s(U)]\sqrt{\nu(t)} \,,$$
$$b_1(t, \tau_1, \tau_2) = \frac{1}{2}\frac{\mathbb{V}[s(U)]}{\mathbb{E}[s(U)]}\sqrt{\nu(t)} \,,$$

for a uniformly distributed random variable $U \sim \mathcal{U}[\tau_1, \tau_2]$. Having option pricing in view, we would like to mention that we again preserve the affine structure of the model, that is as $(\log(F(t, \tau)), \nu(t))$ is affine in the volatility, so is $(\log(F(t, \tau_1, \tau_2)), \nu(t))$ after applying the averaging procedure of Chapter 2.

In Figure 4 the deterministic part of the swaps volatility $S_1(t, \tau_1, \tau_2)$ is plotted as well as the deterministic part of the market price of risk $S_2(t, \tau_1, \tau_2)$. The parameters can be found in Table 2. While $S_1(t, \tau_1, \tau_2)$ is the hightest in the winter and the lowest in the summer, $S_2(t, \tau_1, \tau_2)$ has two peaks in spring and autumn when the changes in $s(u)$ are the biggest.

Table 2 *Parameters for the simulations.*

Joint Parameters								
F_0	ν_0	τ_1	τ_2	ρ	r	κ	σ	θ
30	0.6	0.75	$0.8\overline{3}$	-0.3	0.01	3	0.4	0.6

Seasonality in Trading Days			Samuelson	Seasonality in the Delivery		
α	β	γ	λ	a	b	c
0.6	0.7	0.2	3.5	1	0.4	0

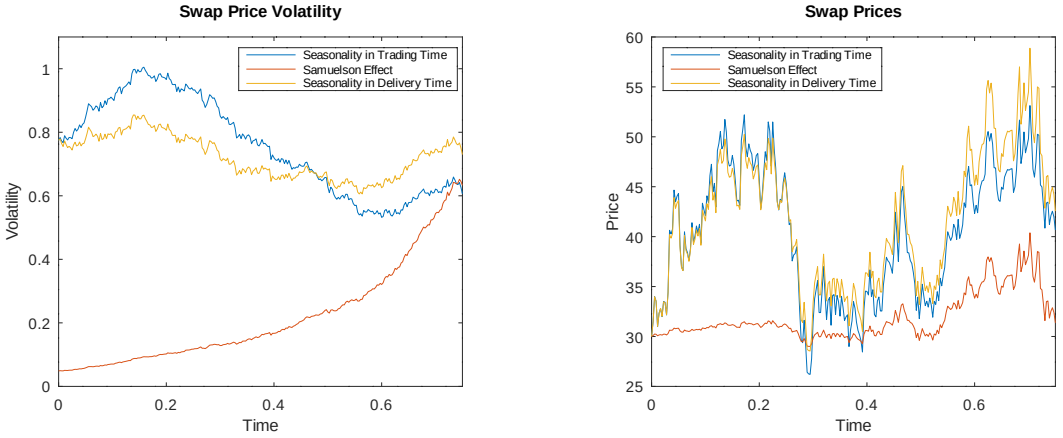

Figure 5 *The swap price volatility $\Sigma(t, \tau_1, \tau_2)$ for each example (left) and swap prices $F(t, \tau_1, \tau_2)$ for each example (right). The trajectories are based on the parameters in Table 2.*

3.4. Comparison of the Models

For our simulation study, we applied the Euler-Maruyama procedure to the swap process and the drift-implicit Milstein procedure to the volatility process. The parameters used in this chapter are summarized in Table 2. For each model, they fulfill the Feller-condition to ensure that the stochastic volatility stays strictly positive as well as the Novikov condition such that the measure change is well defined (see Chapter 3.1–3.3 for details). Note that the initial swap price volatility $\Sigma(0, \tau_1, \tau_2)$ might be different for each model even if the initial value ν_0 of the Cox-Ingersoll-Ross process is always the same. For the parameters in Table 2, the initial swap price volatilities of the two seasonality models are equal since $S_1(\frac{9}{12}, \frac{10}{12}) \approx 1$ (see Figure 4).

In Figure 5, we have plotted the evolution of the stochastic volatility as well as the swap prices of all three considered models both under the measure $\widetilde{\mathbb{Q}}$. For better comparison, we use the same Brownian increments for each model. Our time scale reflects 9 month starting from January with delivery in October. In the red trajectory, we can clearly observe the Samuelson effect, which diminishes

the volatility at the beginning and pushes in the end towards $d_1(\frac{1}{12})\sqrt{\nu(\tau_1)}$. Moreover, the swap price volatility with seasonality in the delivery time is oscillating around the swap price volatility of the first example. This is caused by the choice of parameters since $S_1(\tau_1, \tau_2) \approx 1$ and can be observed both in the swap price volatility and in the swap price trajectory.

4. Further Arbitrage Considerations

So far, we have considered a market with one swap contract. Nevertheless, in electricity markets, typically more than one swap is traded at the same time. For example, at the EEX, the next 9 months, 11 quarters and 6 years are available. In Chapter 4.1, we address the issue of arbitrage in a market consisting of N monthly delivering swaps and then discuss a market with overlapping delivery periods in Chapter 4.2.

4.1. Absence of Arbitrage in a Market with N Swaps

In this chapter, we consider a market with N swap contracts having subsequent monthly delivery periods $(\tau_m, \tau_{m+1}]$ for $m = 1, \ldots, N$. According to the First Fundamental Theorem of Asset Pricing, the market is arbitrage-free if there exists a measure $\widetilde{\mathbb{Q}}$ under which all swap contracts are martingales. In a market with N assets, N Brownian motions are needed such that a market price of risk exists (see, e.g., Shreve (2004)). Therefore, we add another factor for each contract and the underlying futures price dynamics are given by

$$dF(t,\tau) = F(t,\tau)\sum_{j=1}^{N}\sigma_j(t,\tau)dW_j^F(t)\ , \qquad F(0,\tau) = F_0 > 0\ , \tag{4.1}$$

where W_j^F, for $j = 1, \ldots, N$, are independent standard Brownian motions under $\mathbb{Q}$. As in Chapter 2, we define the swap price with delivery period $(\tau_m, \tau_{m+1}]$, for $m = 1, \ldots, N$ via geometric averaging

$$F(t,\tau_m,\tau_{m+1}) := \exp\left(\int_{\tau_m}^{\tau_{m+1}} w(u,\tau_m,\tau_{m+1})\log(F(t,u))du\right)\ .$$

The resulting swap price dynamics for the monthly delivery period $(\tau_m, \tau_{m+1}]$, $m = 1, \ldots, N$ are given by

$$\begin{aligned}\frac{dF(t,\tau_m,\tau_{m+1})}{F(t,\tau_m,\tau_{m+1})} =& \frac{1}{2}\sum_{j=1}^{N}\left(\Sigma_j^2(t,\tau_m,\tau_{m+1}) - \int_{\tau_m}^{\tau_{m+1}} w(u,\tau_m,\tau_{m+1})\sigma_j^2(t,u)du\right)dt \\ &+ \sum_{j=1}^{N}\int_{\tau_m}^{\tau_{m+1}} w(u,\tau_m,\tau_{m+1})\sigma_j(s,u)du\ dW_j^F(t)\ .\end{aligned} \tag{4.2}$$

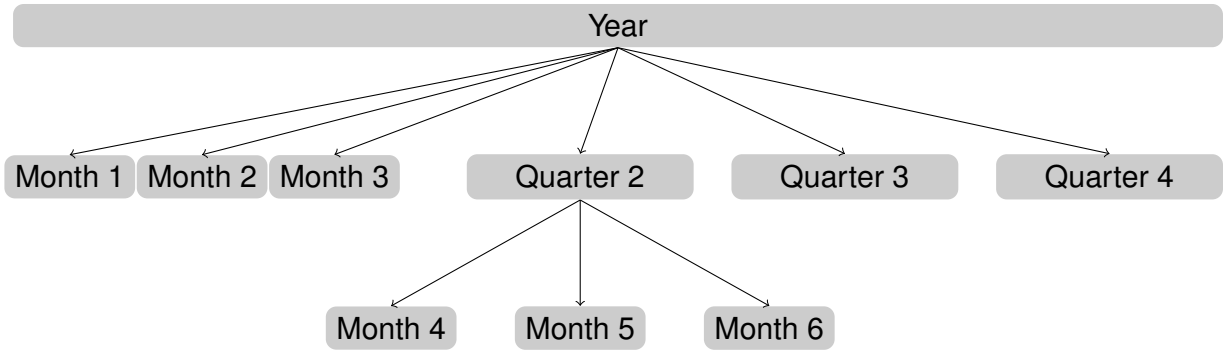

Figure 6 *The cascading procedure of overlapping electricity swap contracts.*

Then the standard theory for multidimensional markets (see, e.g., Shreve (2004)) leads to the market price of risk equations and a risk-neutral probability measure.

4.2. Absence of Arbitrage in a Market with Overlapping Swaps

In electricity markets, it is possible to trade into overlapping delivery periods. For example, the swap contract on the next quarter of the year is available as well as the three swaps on the corresponding months. Also here, arbitrage has to be excluded: It should not matter if the electricity is bought via a quarterly contract or the corresponding three underlying monthly contracts.

One has to find a pricing measure under which all contracts, the monthly and the quarterly ones, are martingales. If we would price an overlapping contract using the geometric averaging procedure, we would have that

$$F^{overl}(t,\tau_1,\tau_{N+1}) = e^{\int_{\tau_1}^{\tau_{N+1}} w(u,\tau_1,\tau_{N+1})\log(F(t,u))du} = \prod_{m=1}^{N} F(t,\tau_m,\tau_{m+1})^{w_m} \ ,$$

where $w_m = \frac{\int_{\tau_m}^{\tau_{m+1}} \hat{w}(u)du}{\int_{\tau_1}^{\tau_{N+1}} \hat{w}(u)du}$. The price of the quarterly swap would be the product of the monthly contracts. This might create arbitrage opportunities: In general, the product of martingales is not a martingale anymore. In this framework, the so-called cascading process of overlapping contracts offers a solution. The cascading process describes the division of an overlapping contract into its building blocks. A swap contract delivering over a quarter is transformed into its corresponding monthly swap contracts at its maturity (see Figure 6). Analogously, the price of a yearly swap contract is converted into the first 3 monthly contracts and the subsequent 3 quarterly contracts. Each quarterly contract will be cascaded later. The monthly contracts thus play the role of building blocks for overlapping contracts and are also called atomic contracts. Consequently, the quarterly and yearly swap contracts can be seen derivatives on the monthly contracts, and we propose to price them as such. If we have found a pricing measure under which all atomic swap prices are martingales, then F^{overl} is also a martingale since the sum of $\widetilde{\mathbb{Q}}$-martingales stays a martingale under $\widetilde{\mathbb{Q}}$.

5. Electricity Options

We consider a European call option with strike price $K > 0$ and exercise time $T < \tau_1$ written on an electricity swap contract delivering in $(\tau_1, \tau_2]$. In Chapter 2, we have determined an equivalent measure $\widetilde{\mathbb{Q}}$, such that the swap price $F(\cdot, \tau_1, \tau_2)$ is a martingale. Hence, $\widetilde{\mathbb{Q}}$ can be used as pricing measure for derivatives on the swap. In general, $\widetilde{\mathbb{Q}}$ depends on τ_1 and τ_2 since it includes a risk premium for the delivery period as discussed in Remark 1. Hence, the pricing measure is tailor-made for this particular contract.

5.1. An Application of the Heston-Methodology

Motivated by the market models considered in Chapter 3, we stick to a general factorizing volatility structure $\Sigma(t, \tau_1, \tau_2) = S(t, \tau_1, \tau_2)\sqrt{\nu(t)}$, where

$$S(t, \tau_1, \tau_2) = \mathbb{E}\left[s(t, U)\right] \tag{5.1}$$

identifies averaged seasonalities and term-structure effects for a random variable U with density $w(u, \tau_1, \tau_2)$ (see also Remark 1). We assume that $s(t, u)$ is positive and bounded by R, so that the swap price model

$$\begin{aligned} dF(t, \tau_1, \tau_2) =& S(t, \tau_1, \tau_2)\sqrt{\nu(t)}F(t, \tau_1, \tau_2)d\widetilde{W}^F(t) \,, & (5.2)\\ d\nu(t) =& (\kappa\theta(t) - (\kappa + \sigma\rho\xi(t, \tau_1, \tau_2))\nu(t))\, dt + \sigma\sqrt{\nu(t)}d\widetilde{W}^\sigma(t) \,. & (5.3) \end{aligned}$$

is a $\widetilde{\mathbb{Q}}$-martingale if $2\kappa^2 > \sigma^2 R^2$ (see Appendix B). The market price of delivery risk is given by $b_1(t, \tau_1, \tau_2) = \xi(t, \tau_1, \tau_2)\sqrt{\nu(t)}$, where

$$\xi(t, \tau_1, \tau_2) = \frac{1}{2}\frac{\mathbb{V}\left[s(t, U)\right]}{\mathbb{E}\left[s(t, U)\right]} \,. \tag{5.4}$$

The price of the corresponding electricity call option at time $t \in [0, T]$ is given by the risk-neutral valuation formula

$$C(t, \tau_1, \tau_2) = \mathbb{E}_{\tilde{\mathbb{Q}}}\left[e^{-r(T-t)}\left(F(T, \tau_1, \tau_2) - K\right)^+ |\mathcal{F}_t\right] \,, \tag{5.5}$$

see, e.g., Shreve (2004). The dynamics of the logarithmic swap price $X(t) := \log(F(t, \tau_1, \tau_2))$ are given by

$$dX(t) = -\frac{1}{2}S^2(t, \tau_1, \tau_2)\nu(t)dt + S(t, \tau_1, \tau_2)\sqrt{\nu(t)}d\widetilde{W}^F(t) \,. \tag{5.6}$$

We skip the dependencies on the delivery period for notational convenience. We thus have the following result:

Theorem 1. *The electricity option price at time $t \leq T$ with strike price $K > 0$ is given by*

$$C(t, \tau_1, \tau_2) = e^{-r(T-t)} \left(e^x \left(1 - Q_1(t, x, \nu; \log(K)) \right) - K \left(1 - Q_2(t, x, \nu; \log(K)) \right) \right) , \tag{5.7}$$

where the probabilities of exercising the option are given by

$$1 - Q_k(t, x, \nu; \log(K)) = \frac{1}{2} + \frac{1}{\pi} \int_0^\infty Re \left(\frac{e^{-i\phi \log(K)} \hat{Q}_k(t, x, \nu; \phi)}{i\phi} \right) d\phi , \quad k = 1, 2 . \tag{5.8}$$

The characteristic functions $\hat{Q}_k(t, x, \nu; \phi)$ are given by

$$\hat{Q}_k(t, x, \nu; \phi) = e^{\Psi_{0k}(t,T,\phi) + \nu \Psi_{1k}(t,T,\phi) + i\phi x} , \qquad k = 1, 2 , \tag{5.9}$$

where $\Psi_{0k}(t, T, \phi)$ and $\Psi_{1k}(t, T, \phi)$ solve the following system of differential equations

$$\frac{\partial \Psi_{1k}}{\partial t} = -\frac{1}{2}\sigma^2 \Psi_{1k}^2 + \left(\beta_k(t, \tau_1, \tau_2) - \rho\sigma S(t, \tau_1, \tau_2) i\phi \right) \Psi_{1k} + \left(\frac{1}{2}\phi^2 - \alpha_k i\phi \right) S^2(t, \tau_1, \tau_2) , \tag{5.10}$$

$$\frac{\partial \Psi_{0k}}{\partial t} = -\Psi_{1k} \kappa\theta(t) , \tag{5.11}$$

for $\alpha_1 = \frac{1}{2}$, $\alpha_2 = -\frac{1}{2}$, $\beta_1(t, \tau_1, \tau_2) = \kappa + \sigma\rho(\xi(t, \tau_1, \tau_2) - S(t, \tau_1, \tau_2))$, $\beta_2(t, \tau_1, \tau_2) = \kappa + \sigma\rho\xi(t, \tau_1, \tau_2)$.

The proof follows the Heston procedure and can be found in Appendix C. There exists a unique solution to each Riccati equation (see Appendix D) and thus also for Ψ_{01} and Ψ_{02}. Then, the characteristic functions in (5.9) are uniquely determined. The related put option price can be determined by the *Put-Call-Parity*.

The value of this result depends strongly on the tractability of the Riccati equations (5.10). In the classical Heston model, all coefficients of the Riccati equations (5.10) are constant, so that one can find an analytical solution. For time-dependent coefficients, it is not clear that an analytical solution or closed-form expression exists. In Arismendi et al. (2016), the mean reversion level $\theta(t)$ of the stochastic volatility process is seasonal, but as $\theta(t)$ does not appear in the Riccati equation, an analytical solution exists. Schneider and Tavin (2018) include the Samuelson effect such that the futures price dynamics have time-dependent coefficients. Nevertheless, the volatility process has constant coefficients. The Samuelson term appears in the Riccati equations and Schneider and Tavin (2018) are able to give a solution depending on Kummer functions. In our framework, the Samuelson effect appears in the drift of the stochastic volatility via the market price of delivery risk, making the Riccati equations more complicated (see Chapter 5.2.2).

5.2. The Effect of Seasonalities and Samuelson on the Swaps' Riccati Equation

In this chapter, we state the differential equations (5.10) and (5.11) for each model, and discuss how to solve them. Furthermore, we compare the corresponding option prices numerically. Let us mention, that for the classical Riccati equation setting, which corresponds to the Heston model with constant coefficients, the exact formula for the solution can be found easily. In general, the equation has to be solved numerically. We discuss this situation in the subsequent sections.

5.2.1. Seasonal Dependence on the Trading Day

In the setting of (3.3) and (3.4), option pricing has been treated by Arismendi et al. (2016). Recall, that $\Psi_{0k}(t,T,\phi)$ and $\Psi_{1k}(t,T,\phi)$ solve the following system of differential equations

$$\begin{aligned}\frac{d\Psi_{1k}}{dt}(t,T,\phi) =& -\frac{1}{2}\sigma^2\Psi_{1k}^2(t,T,\phi) + (\beta_k - \rho\sigma i\phi)\,\Psi_{1k}(t,T,\phi) + \frac{1}{2}\phi^2 - \alpha_k i\phi\ ,\\ \frac{d\Psi_{0k}}{dt}(t,T,\phi) =& -\kappa\theta(t)\Psi_{0k}(t,T,\phi)\ ,\end{aligned}$$

for $\alpha_1 = \frac{1}{2}$, $\alpha_2 = -\frac{1}{2}$, $\beta_1 = \kappa - \sigma\rho$, and $\beta_2 = \kappa$. Since all coefficients of the Riccati equations (the first equation of the system) are constant, the solutions can be calculated by

$$\Psi_{1k}(t,T,\phi) = \frac{1}{\sigma^2}\left(\beta_k - \sigma\rho\phi i - \delta_k\right)\frac{1-e^{-\delta_k(T-t)}}{1-g_k e^{-\delta_k(T-t)}}\ , \quad k=1,2\ ,$$

where

$$\begin{aligned}\delta_k :=& \sqrt{(\beta_k - \sigma\rho\phi i)^2 + 2\sigma^2(\frac{1}{2}\phi^2 - \alpha_k\phi i)}\ ,\\ g_k :=& \frac{\beta_k - \sigma\rho\phi i - \delta_k}{\beta_k - \sigma\rho\phi i + \delta_k}\ .\end{aligned}$$

Finally, numerical integration leads to the solution of $\Psi_{01}(t,T,\phi)$ and $\Psi_{02}(t,T,\phi)$ (see Chapter 5.2.4).

In Figure 7, we illustrate the option prices for different speed of mean-reversion parameters ($\kappa = 0.6$, $\kappa = 3$, and $\kappa = 10$) over the entire time horizon based on the parameters in Table 2 and 3. The calculations are conducted by using the analytical solution for the Riccati equations. The solutions for Ψ_{0k} are attained using the Runge-Kutta method. We here require a relative and absolute tolerance of $1e-8$. As proposed by Arismendi et al. (2016), we apply a trapezoidal integration scheme to obtain the integral values for each strike which are mandatory to determine the corresponding probabilities $1-Q_1$ and $1-Q_2$ as in (5.8) and thus the related option price for the considered strike at a specific point in time (see (5.7)). As a result, we can observe decreasing call option prices over time. Moreover, the lower the speed of mean-reversion, the higher is the option price except for the first trading days.

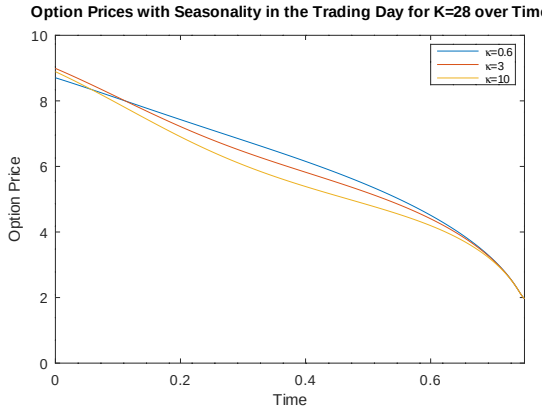

Figure 7 *Option prices with seasonality in the trading day over the whole time horizon for a fixed strike $K = 28$.*

The closer we reach the expiration date, the smaller is the difference between each option price for a fixed strike price.

5.2.2. Samuelson Effect

In the setting of Chapter 3.2, the resulting dynamics under $\widetilde{\mathbb{Q}}$ are given by (3.12) and (3.13). Under the measure $\widetilde{\mathbb{Q}}$, the Samuelson effect appears in the drift term of the stochastic volatility.

$\Psi_{0k}(t,T,\phi)$ and $\Psi_{1k}(t,T,\phi)$ for $k = 1,2$ solve the following two systems of differential equations:

$$\begin{aligned}
\frac{d\Psi_{11}}{dt}(t,T,\phi) =& -\frac{1}{2}\sigma^2\Psi_{11}^2(t,T,\phi)+ \\
&\Big(\kappa+\sigma\rho\Big[d_2(\tau_2-\tau_1)-d_1(\tau_2-\tau_1)(1+i\phi)\Big]e^{-\lambda(\tau_1-t)}\Big)\Psi_{11}(t,T,\phi) \\
&+\frac{1}{2}d_1(\tau_2-\tau_1)^2(\phi^2-i\phi)e^{-2\lambda(\tau_1-t)}\ , \\
\frac{d\Psi_{01}}{dt}(t,T,\phi) =& -\kappa\theta\Psi_{11}(t,T,\phi)\ ,
\end{aligned}$$

and

$$\begin{aligned}
\frac{d\Psi_{12}}{dt}(t,T,\phi) =& -\frac{1}{2}\sigma^2\Psi_{12}^2(t,T,\phi) \\
&+\Big(\kappa+\sigma\rho\Big[d_2(\tau_2-\tau_1)-i\phi d_1(\tau_2-\tau_1)\Big]e^{-\lambda(\tau_1-t)}\Big)\Psi_{12}(t,T,\phi) \\
&+\frac{1}{2}d_1(\tau_2-\tau_1)^2(\phi^2+i\phi)e^{-2\lambda(\tau_1-t)}\ , \\
\frac{d\Psi_{02}}{dt}(t,T,\phi) =& -\kappa\theta\Psi_{12}(t,T,\phi)\ ,
\end{aligned}$$

where $d_1(x)$ and $d_2(x)$ are defined in (3.11). Compared to Schneider and Tavin (2018), the Samuelson

effect appears additionally in front of Ψ_{11} and Ψ_{12}. This leads to the setting of time-dependent coefficients in the Riccati-type equations. The explicit solution is expressed in terms of hypergeometric expressions.

Figure 8 illustrates option prices with respect to seven strike prices based on the default parameters introduced in Table 2 and 3. We use the Runge-Kutta method with adaptive step size to solve both systems of differential equations. The trapezoidal integration of the integrands with respect to ϕ leads to the cumulative distributions Q_1 and Q_2 for each strike price K. An application of Equation (5.7) gives the corresponding option prices for each strike. In fact, we approximate the analytic expressions for Ψ_{11}, Ψ_{12}, Ψ_{01}, and Ψ_{02} since two coefficients in the Riccati equation include the Samuelson effect.

For models with time-dependent θ, σ, and ρ, the method by Benhamou et al. (2010) can be applied with the help of a volatility of variance expansion using the Lewis representation. For time-dependent coefficients of piece-wise constant structure, one can also use the model of Mikhailov and Nögel (2004). However, in general, the solution has to be found numerically. Most of them concern the one dimensional case, for example, standard second order finite difference methods, see Tavella and Randall (2000). More recently, results include stochastic volatility with high-order compact finite difference schemes such as Crank–Nicolson scheme, see Düring et al (2014).

In order to investigate the impact of the Samuelson effect, we set the parameter λ to 1.5, 3.5, and 5.5. As a result, we observe higher option prices for smaller Samuelson parameters, which are decreasing in increasing strike prices. The differences are especially large for at the money strikes. With increasing time to maturity, these differences become even larger. To add, the option prices become more affeced the closer we reach the expiration date (see Figure 8 (right)).

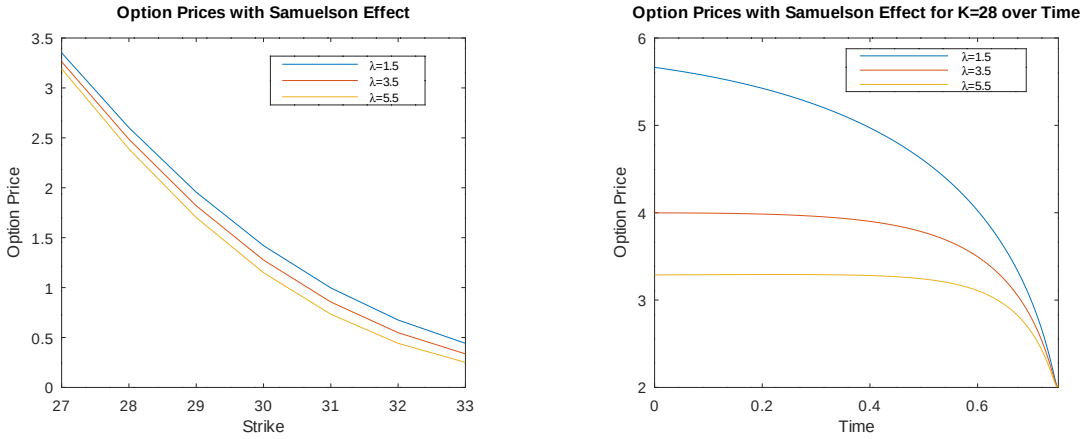

Figure 8 *Option prices with Samuelson effect 10 days before maturity (left) and over the entire time horizon for a fixed strike $K = 28$ (right).*

5.2.3. *Delivery-Dependent Seasonality*

Finally, we consider the resulting option prices corresponding to Chapter 3.3. $\Psi_{0k}(t,T,\phi)$ and $\Psi_{1k}(t,T,\phi)$ for $k=1,2$ solve the following two systems of differential equations:

$$\begin{aligned}\frac{d\Psi_{11}}{dt}(t,T,\phi) =& -\frac{1}{2}\sigma^2\Psi_{11}^2(t,T,\phi) + \Big(\kappa + \sigma\rho\Big[S_2(\tau_1,\tau_2) - S_1(\tau_1,\tau_2)(1+i\phi)\Big]\Big)\Psi_{11}(t,T,\phi)\\ &+\frac{1}{2}S_1(\tau_1,\tau_2)^2(\phi^2 - i\phi)\ ,\\ \frac{d\Psi_{01}}{dt}(t,T,\phi) =& -\kappa\theta\Psi_{11}(t,T,\phi)\ ,\end{aligned}$$

and

$$\begin{aligned}\frac{d\Psi_{12}}{dt}(t,T,\phi) =& -\frac{1}{2}\sigma^2\Psi_{12}^2(t,T,\phi) + \Big(\kappa + \sigma\rho\Big[S_2(\tau_1,\tau_2) - i\phi S_1(\tau_1,\tau_2)\Big]\Big)\Psi_{12}(t,T,\phi)\\ &+\frac{1}{2}S_1(\tau_1,\tau_2)^2(\phi^2 + i\phi)\ ,\\ \frac{d\Psi_{02}}{dt}(t,T,\phi) =& -\kappa\theta\Psi_{12}(t,T,\phi)\ .\end{aligned}$$

The differential equations can be solved analytically, while all coefficients are constant. The solutions are given by

$$\Psi_{1k}(t,T,\phi) = \frac{1}{\sigma^2}\left(\beta_k(\tau_1,\tau_2) - \sigma\rho\phi i - \delta_k(\tau_1,\tau_2)\right)\frac{1-e^{-\delta_k(\tau_1,\tau_2)(T-t)}}{1-g_k(\tau_1,\tau_2)e^{-\delta_k(\tau_1,\tau_2)(T-t)}}\ , \tag{5.12}$$

where

$$\begin{aligned}\beta_1(\tau_1,\tau_2) =& \kappa + \sigma\rho(S_2(\tau_1,\tau_2) - S_1(\tau_1,\tau_2))\ ,\\ \beta_2(\tau_1,\tau_2) =& \kappa + \sigma\rho S_2(\tau_1,\tau_2)\ ,\\ \delta_k(\tau_1,\tau_2) :=& \sqrt{(\beta_k(\tau_1,\tau_2) - \sigma\rho\phi i)^2 + 2\sigma^2(\frac{1}{2}\phi^2 - \alpha_k\phi i)}\ ,\\ g_k(\tau_1,\tau_2) :=& \frac{\beta_k(\tau_1,\tau_2) - \sigma\rho\phi i - \delta_k(\tau_1,\tau_2)}{\beta_k(\tau_1,\tau_2) - \sigma\rho\phi i + \delta_k(\tau_1,\tau_2)}\ ,\end{aligned}$$

and

$$\begin{aligned}\Psi_{0k}(t,T,\phi) = -\frac{\kappa\theta}{\sigma^2}\Big[&\Big(\beta_k(\tau_1,\tau_2) - \sigma\rho\phi i - \delta_k(\tau_1,\tau_2)\Big)(T-t)\\ &-2\log\left(\frac{1-g_k(\tau_1,\tau_2)e^{-\delta_k(\tau_1,\tau_2)(T-t)}}{1-g_k}\right)\Big]\ .\end{aligned}$$

The delivery dependent seasonality model is able to incorporate delivery dependent effects, while being highly tractable and fast to implement. In Figure 9, we visualize the option prices over the last

Figure 9 *Option prices with seasonality in the delivery over the last trading month for fixed strikes.*

Table 3 *Parameters for pricing options.*

Parameters					
T	K	Iterations	ϕ_{min}	ϕ_{max}	n
0.75	$27, \ldots, 33$	100	0.0000001	75	1.000.000

trading month based on the parameters in Table 2 and 3. For the calculations, we use the analytical solutions for $\Psi_{01}, \Psi_{02}, \Psi_{11}$, and Ψ_{12}. As before, numerical integration leads to the desired option price for each considered strike.

As a result, the option prices are decreasing with an increasing strike price. Furthermore, the option prices are decreasing over time for all strikes.

5.2.4. Numerical Comparison of the Effects

In this chapter, we focus on concrete numerical examples based on the transformed models in Chapter 3 and Chapter 5.2. We consider the integrands for each model as well as the resulting call option prices. For comparative reasons, we have chosen the same parameters for all examples (see Table 2 and 3). In order to determine both integrands for each model, we calculate the solution to the system of ordinary differential equations as in Chapter 5.2.1–5.2.2. We used the analytical solution of the Riccati equations with seasonality in the trading day and in the delivery time. We get a certain integrand depending on ϕ for each strike price. The possible oscillation of the integrand can have a negative influence on the numerical procedure since the standard quadrature can fail, see Rouah (2013). We can observe that both integrands are relatively smooth for each model and converge to zero around $\phi \approx 50$ (see Figure 10). For the integration, we apply the standard trapezoidal rule. To be precise, we fix the upper boundary for the integrands with $\phi_{max} = 100$ due to the converting behavior and truncate the lower boundary at $\phi_{min} = 0.0000001$. Plugging the integral value into (5.8) leads to the option

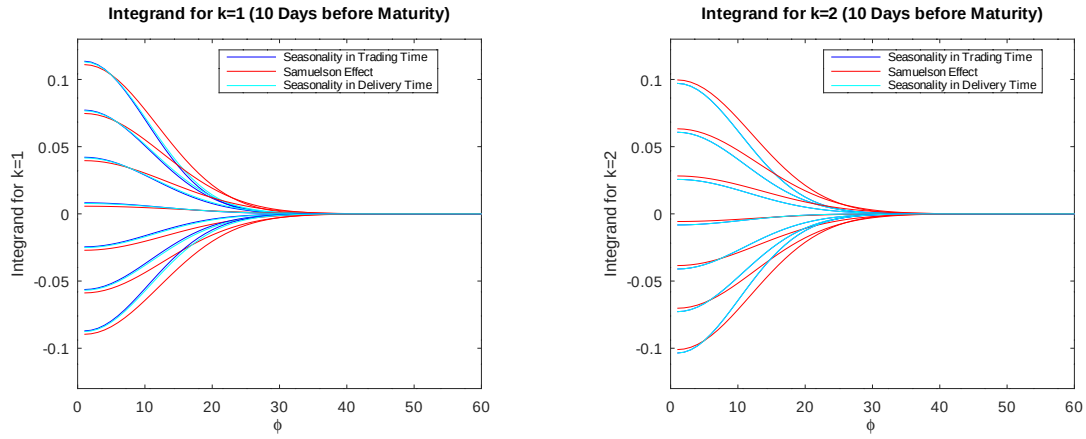

Figure 10 *Integrands for each model and for all strikes $K = 27, \ldots, 33$.*

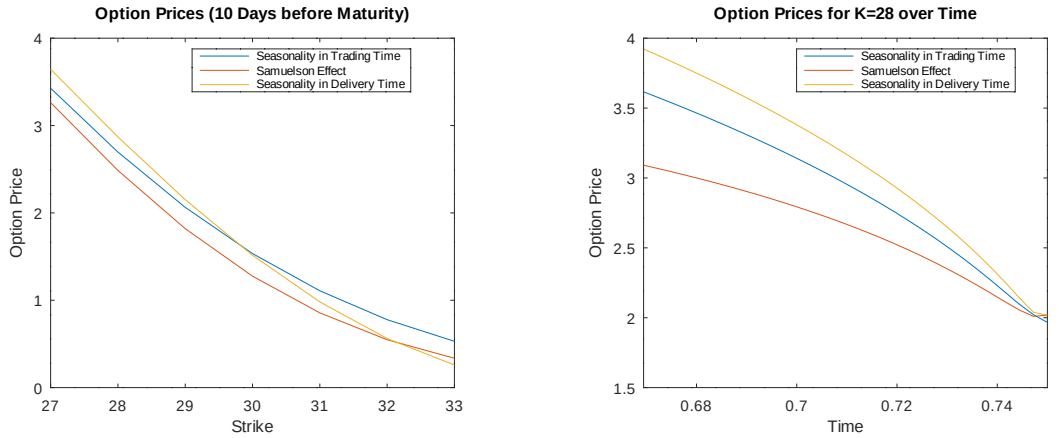

Figure 11 *Option prices for each model 10 days before maturity (left) and over the last trading month for a fixed strike $K = 28$ (right). The parameters are based on Table 2 and 3.*

prices (5.7) (see Figure 11 (left)). To compare the resulting prices, we also conduct a simulation study based on the parameters in Table 3 starting 20 days before the swap contract expires. The results can be found in Figure 11 (right). In all examples, we observe decreasing option prices for increasing strikes. An application of the Samuelson effect leads to smaller option prices than in the first example with seasonality in the trading time. Seasonality in the delivery leads to higher option prices for out of the money strikes than in the case of the first example. Only for far in the money strikes, the option prices are even smaller than the ones resulting from the Samuelson effect. Having the last trading month in view, the option prices are decreasing in time. For the fixed strike $K = 28$, the option prices for the Samuelson effect the smallest. In contrast, seasonalities in the delivery affect the option prices at most so that they show the highest option prices over the last trading month.

6. Conclusion

We suggest the use of a pricing framework for swaps and options in electricity markets. Moreover, we introduced an equivalent martingale measure for the swap that explicitly depends on its delivery period and can be used to price electricity options. Geometric averaging on the delivery period is the key element here. The market price of delivery risk for an individual contract is specified by the trade-off between the variance of the swap on the one hand and the weighted average variance of a stream of futures on the other hand. We considered futures price models from the recent literature and provide the corresponding swap price models. Moreover, we investigated the effect of seasonal dependence on the trading day, the Samuelson effect, and delivery-dependent seasonality in line with Arismendi et al. (2016), Schneider and Tavin (2018), and Fanelli and Schmeck (2019), respectively. Whenever the futures and thus the swap price volatility are independent of the delivery time, the market price of delivery risk is zero. On the other hand, typically observed characteristics of the electricity market, such as seasonalities in the delivery and term-structure effects, instead impact the market price of the delivery risk.

Moreover, we provided an outlook of our model in the case of several atomic and overlapping contracts. For each additional atomic contract, new uncertainty occurs, and a further Brownian motion is thus needed within the futures price. The pricing procedure can be applied as before. Overlapping contracts are treated as derivatives of the underlying atomic swap contracts, which is justified by the cascading process (see Figure 6).

All examples are characterized by a volatility structure in the spirit of the Heston model. The affine model structure of the futures is inherited by the swaps, thereby leading us to follow the Heston methodology for option pricing. We investigated the option price for seasonal dependence on the trading day, the Samuelson effect, and delivery-dependent seasonality. Whenever the deterministic volatility part is independent of the trading time, the corresponding Riccati equations can be solved analytically. For the Samuelson effect, the deterministic part of the volatility is time-dependent, and we showed that a unique solution exists. Furthermore, we provided a numerical method to solve the Riccati equations.

In conclusion, this paper treats each electricity swap as a proper contract on the market and suggests a pricing measure that is tailor-made for this particular contract, which includes acknowledging the existence of the delivery period. Our pricing framework allows for the evaluation of option prices in line with the Heston method.

References

ARISMENDI, J. C., BACK, J., PROKOPCZUK, M., PASCHKE, R., AND RUDOLF, M. (2016). Seasonal Stochastic Volatility: Implications for the Pricing of Commodity Options. *Journal of Banking and Finance* **66**, pp. 53-65.

BENHAMOU, E., GOBET, E., AND MIRI, M. (2010). Time-Dependent Heston Model. *SIAM Journal on Financial Mathematics* **1**(1), pp. 289-325.

BENTH, F. E., BENTH, J. S., AND KOEKEBAKKER, S. (2008). Stochastic Modelling of Electricity and Related Markets. Vol. 11. *World Scientific Publishing Company*.

BENTH, F. E., PICCIRILLI, M., AND VARGIOLU, T. (2019). Mean-Reverting Additive Energy Forward Curves in a Heath–Jarrow–Morton Framework. *Mathematics and Financial Economics*, pp. 1-35.

BENTH, F. E. AND SCHMECK, M. D. (2014). Pricing futures and options in electricity markets. In: *The Interrelationship Between Financial and Energy Markets*, edited by Sofia Ramos and Helena Veiga, pp. 233-260, (Springer: Berlin).

BJERKSUND, P., RASMUSSEN, H., AND STENSLAND, G. (2010). Valuation and Risk Management in the Norwegian Electricity Market. *Energy, Natural Resources and Environmental Economics*, pp. 167-185.

BOROVKOVA, S. AND SCHMECK, M. D. (2017). Electricity Price Modeling with Stochastic Time Change. *Energy Economics* **63**, pp. 51-65.

CONT, R. AND TANKOV, P. (2004). Financial Modelling with Jump Processes. *Chapman and Hall/CRC*.

DUFFIE, J. D. (2010). Dynamic Asset Pricing Theory. *Princeton University Press*.

DÜRING, B., MICHEL FOURNIÉ, M., AND HEUER, C. (2014). High-order Compact Finite Difference Schemes for Option Pricing in Stochastic Volatility Models on Non-Uniform Grids. *Journal of Computational and Applied Mathematics* **271**, pp. 247-266.

FANELLI, V. AND SCHMECK, M. D. (2019). On the Seasonality in the Implied Volatility of Electricity Options. *Quantitative Finance*, pp. 1-17.

GIL-PELAEZ, J. (1951). Note on the Inversion Theorem. *Biometrika* **38**, pp. 481-482.

HESTON, S. L. (1993). A Closed-Form Solution for Options with Stochastic Volatility with Applica-

tions to Bond and Currency Options. *The Review of Financial Studies* **6**(2), pp. 327-343.

KARATZAS, I. AND SHREVE, S. E. (1991). Brownian Motion and Stochastic Calculus. *Springer*; 2nd edition.

KEMNA, A. G. Z. AND VORST, A. C. F. (1990). A Pricing Method for Options based on Average Asset Values. *Journal of Banking and Finance* **14**(1), pp. 113-129.

KIESEL, R., SCHINDLMAYR, G., AND BÖRGER, R. H. (2009). A Two-Factor Model for the Electricity Forward Market. *Quantitative Finance* **9**, 279-287.

MIKHAILOV, S. AND NÖGEL, U. (2004). Heston's Stochastic Volatility Model Implementation, Calibration and Some Extensions. *John Wiley and Sons*.

POLJANIN, A. D. AND ZAJCEV, V. F. (2018). Handbook of Ordinary Differential Equations. *CRC Press*.

PROTTER, P. E. (2005). Stochastic Differential Equations. *Stochastic Integration and Differential Equations*. Springer, pp. 249-361.

ROUAH, F. D. (2013). The Heston Model and Its Extensions in Matlab and C#. *John Wiley & Sons*.

SAMUELSON, P. A. (1965). Proof that Properly Anticipated Prices Fluctuate Randomly. *Industrial Management Review* **6**(2), pp. 41–49.

SCHMECK, M. D. (2016). Pricing Options on Forwards in Energy Markets: the Role of Mean Reversions Speed. *International Journal of Theoretical and Applied Finance* **19**(8), 1650053.

SCHNEIDER, L. AND TAVIN, B. (2018). From the Samuelson Volatility Effect to a Samuelson Correlation Effect: An Analysis of Crude Oil Calendar Spread Options. *Journal of Banking and Finance* **95**, pp. 185–202.

SHREVE, S. E. (2004). Stochastic Calculus for Finance II. Continuous-Time Models. *Springer Finance Series*.

TAVELLA, D., AND RANDALL, C. (2000). Pricing Financial Instruments: The Finite Difference Method. Vol 13. *John Wiley & Sons*.

WALTER, W. (1996). Gewöhnliche Differentialgleichungen. 6th ed. *Springer*.

Appendix

A. Technical Requirements

1. For the model (2.1) and (2.2), we make the following assumtions:

   (a) The conditions by Yamada and Watanabe need to be satisfied (see also Karatzas and Shreve (1991); Proposition 2.13). In particular, we assume

   $$a(t,\tau,\sigma)\colon [0,\tau_1]\times(\tau_1,\tau_2]\times\mathbb{R}^+\to\mathbb{R}\,,$$
   $$c(t,\tau,\sigma)\colon [0,\tau_1]\times(\tau_1,\tau_2]\times\mathbb{R}^+\to\mathbb{R}\,,$$

   are Borel-measurable functions and $\sigma^2 = \{\sigma^2(t,\tau) \mid 0 \le t \le \tau \le \tau_2\}$ is a stochastic process with continuous sample paths. Further, we assume

   - $|a(t,\tau,x) - a(t,\tau,y)| \le K|x-y|$ for some positive constant $K > 0$ with $x, y \in \mathbb{R}^+$,
   - $|c(t,\tau,x) - c(t,\tau,y)| \le H(|x-y|)$ for $x, y \in \mathbb{R}^+$ where $H\colon [0,\infty) \to [0,\infty)$ is an increasing function with $H(0) = 0$ and $\int_{(0,\epsilon)} H^{-2}(u)du = \infty,\ \forall\epsilon > 0$,

   which guarantees that there exists a unique strong solution for (2.2). In particular, $\sigma^2(t,\tau)$ is adapted to the filtration $\mathcal{F}_t$.

   (b) Next, we assume that $F = \{F(t,\tau) \mid 0 \le t \le \tau \le \tau_2\}$ is a stochastic process with continous sample paths. It directly follows that $\sigma(t,\tau)F(t,\tau)$ is process Lipschitz and thus functional Lipschitz. Then, by Protter (2005) (see Theorem 7; p. 253) Equation (2.1) admits a unique strong solution.

   (c) In order to attain that (2.1) is a $\mathbb{Q}$-martingale, we assume that the Novikov condition (see, e.g., Karatzas and Shreve (1991); Proposition 5.12) is satisfied, that is

   $$\mathbb{E}_{\mathbb{Q}}\left[e^{\frac{1}{2}\int_0^\tau \sigma^2(t,\tau)dt}\right] < \infty\,. \tag{A.1}$$

2. For the geometric weightening approach (2.8) we need to apply the stochastic Fubini Theorem (see Protter (2005); Theorem 65; Chapter IV. 6). Therefore, we assume that

   - $(t,u,\omega) \to w(u,\tau_1,\tau_2)\sigma(t,u)$ is jointly progressivly measurable,
   - $\mathbb{E}_{\mathbb{Q}}\left[\int_0^{\tau_1}\int_{\tau_1}^{\tau_2} w^2(u,\tau_1,\tau_2)\sigma^2(t,u)du\,dt\right] < \infty\,.$

B. *An Application of Girsanov's Theorem for the Examples*

We want to check if Novikov's condition is satisfied, that is $\mathbb{E}_{\mathbb{Q}}\left[e^{\frac{1}{2}\int_0^{\tau_1} b_1^2(t,\tau_1,\tau_2)dt}\right] < \infty$ (see, e.g., Karatzas and Shreve (1991)).

In the case of Schneider and Tavin (2018), we can find specific upper and lower boundaries for the deterministic part since $e^{-\lambda(\tau_1-t)} \in [0,1]$ and $d_2(\tau_2-\tau_1) \in [-\frac{1}{2}\frac{1}{\lambda(\tau_2-\tau_1)}, \frac{1}{2}]$. Hence,

$$\mathbb{E}_{\mathbb{Q}}\left[e^{\frac{1}{2}\int_0^{\tau_1} b_1^2(t,\tau_1,\tau_2)dt}\right] = \mathbb{E}_{\mathbb{Q}}\left[e^{\frac{1}{2}\int_0^{\tau_1} d_2(\tau_2-\tau_1)^2 e^{-2\lambda(\tau_1-t)}\nu(t)dt}\right] \leq \mathbb{E}_{\mathbb{Q}}\left[e^{-\tilde{u}\int_0^{\tau_1}\nu(t)dt}\right] , \tag{B.1}$$

where $\tilde{u} := -\frac{1}{8}\max\{1; \frac{1}{\lambda^2(\tau_2-\tau_1)^2}\}$. Following Cont and Tankov (2004) (see Chapter 15.1.2) there exists an explicit, finite expression for the last expectation if $\kappa^2 + 2\sigma^2\tilde{u} > 0$.

In the case of Fanelli and Schmeck (2019), we can again find specific upper and lower boundaries for (3.17) since $s(u) = a + b\cos(2\pi(c+u)) \in [0, 2a]$ for $a > b > 0$ and thus $s^2(u) \leq 2a\ s(u)$. In particular, $S_2(\tau_1,\tau_2) \in [-a, a]$. Hence,

$$\mathbb{E}_{\mathbb{Q}}\left[e^{\frac{1}{2}\int_0^{\tau_1} b_1^2(t,\tau_1,\tau_2)dt}\right] = \mathbb{E}_{\mathbb{Q}}\left[e^{\frac{1}{2}\int_0^{\tau_1} S_2(\tau_1,\tau_2)^2\nu(t)dt}\right] \leq \mathbb{E}_{\mathbb{Q}}\left[e^{-\tilde{u}\int_0^{\tau_1}\nu(t)dt}\right] , \tag{B.2}$$

where $\tilde{u} := -\frac{1}{2}a^2$. As before, the last expectation is limited if $\kappa^2 + 2\sigma^2\tilde{u} > 0$, i.e. $\kappa^2 > a^2\sigma^2$.

In the general case of Chapter 5, we assume that $s(t,u)$ is positive and bounded. As $s(t,u) \in [0,R]$, $\xi(t,\tau_1,\tau_2) \in [-\frac{1}{2}R, \frac{1}{2}R]$. Hence,

$$\mathbb{E}_{\mathbb{Q}}\left[e^{\frac{1}{2}\int_0^{\tau_1} b_1^2(t,\tau_1,\tau_2)dt}\right] = \mathbb{E}_{\mathbb{Q}}\left[e^{\frac{1}{2}\int_0^{\tau_1} \xi(t,\tau_1,\tau_2)^2\nu(t)dt}\right] \leq \mathbb{E}_{\mathbb{Q}}\left[e^{-\tilde{u}\int_0^{\tau_1}\nu(t)dt}\right] , \tag{B.3}$$

where $\tilde{u} := -\frac{1}{4}R^2$. As before, if $\kappa^2 + 2\sigma^2\tilde{u} > 0$, that is if $2\kappa^2 > R_2^2\sigma^2$, then Novikov's condition is satisfied.

C. *Proof of Theorem 1*

Proof. We can write

$$C(t,\tau_1,\tau_2,) = e^{-r(T-t)}\mathbb{E}_{\widetilde{\mathbb{Q}}}\left[e^{X_t}\mathbb{1}_{X_T\geq\log(K)}|\mathcal{F}_t\right] - e^{-r(T-t)}K\ \mathbb{E}_{\widetilde{\mathbb{Q}}}\left[\mathbb{1}_{X_T\geq\log(K)}|\mathcal{F}_t\right] . \tag{C.1}$$

Due to the Markovian structure, an application of the *Independence Lemma* (see, e.g., Shreve (2004); cf. Lemma 2.3.4) leads to

$$C(t,\tau_1,\tau_2) = c_1(t,X(t),\nu(t)) - c_2(t,X(t),\nu(t)) ,$$

where

$$c_1(t,x,\nu) = e^{-r(T-t)}e^x\,(1-Q_1(t,x,\nu;\log(K)))\,, \tag{C.2}$$
$$c_2(t,x,\nu) = e^{-r(T-t)}K\,(1-Q_2(t,x,\nu;\log(K)))\,, \tag{C.3}$$

and

$$Q_1(t,x,\nu;\log(K)) := \tilde{\tilde{\mathbb{Q}}}\left[X^{t,x,\nu}(T)\le\log(K)\right]\,,$$
$$Q_2(t,x,\nu;\log(K)) := \tilde{\mathbb{Q}}\left[X^{t,x,\nu}(T)\le\log(K)\right]\,,$$

where the probability measure $\tilde{\tilde{\mathbb{Q}}}$ is defined by $\frac{d\tilde{\tilde{\mathbb{Q}}}}{d\tilde{\mathbb{Q}}} = e^{-\frac{1}{2}\int_0^T S^2(u,\tau_1,\tau_2)\nu(u)du+\int_0^T S(u,\tau_1,\tau_2)\sqrt{\nu(u)}dW^F(u)}$.

For $k=1,2$, $e^{-rt}c_k(t,X(t),\nu(t))$ are martingales under $\tilde{\mathbb{Q}}$. Hence, $c_k(t,x,\nu)$ solves

$$\frac{\partial c_k(t,x,\nu)}{\partial t} + (\mathcal{A}_t c_k)(t,x,\nu) = r c_k(t,x,\nu), \quad \text{for } k=1,2, \tag{C.4}$$

subject to the terminal conditions $c_1(T,x,\nu) = e^x \mathbb{1}_{x\ge\log(K)}$ and $c_2(T,x,\nu) = K\mathbb{1}_{x\ge\log(K)}$, by an application of the discounted Feynman Kac Theorem (see, e.g., Shreve (2004); cf. Theorem 6.4.3 and Ch. 6.6). For a function f depending on x and ν, the generator of (X,ν) is given by

$$\begin{aligned}(\mathcal{A}_t f)(x,\nu) = &-\frac{1}{2}\frac{\partial f}{\partial x}S^2(t,\tau_1,\tau_2)\nu + \frac{\partial f}{\partial \nu}[\kappa\theta(t) - (\kappa+\sigma\rho\xi(t,\tau_1,\tau_2))\nu] \\ &+\frac{1}{2}\frac{\partial^2 f}{(\partial x)^2}S^2(t,\tau_1,\tau_2)\nu + \frac{1}{2}\frac{\partial^2 f}{(\partial\nu)^2}\sigma^2\nu + \frac{\partial^2 f}{\partial x\partial\nu}\rho\sigma S(t,\tau_1,\tau_2)\nu\,.\end{aligned} \tag{C.5}$$

If we plug (C.2) and (C.3) inside the partial differential equation (PDE) (C.4), we end up with

$$\begin{aligned}&\frac{\partial Q_k}{\partial t} + \alpha_k S^2(t,\tau_1,\tau_2)\nu\frac{\partial Q_k}{\partial x} + (\kappa\theta(t) - \beta_k(t,\tau_1,\tau_2)\nu)\frac{\partial Q_k}{\partial\nu} \\ &+\frac{1}{2}S^2(t,\tau_1,\tau_2)\nu\frac{\partial^2 Q_k}{(\partial x)^2} + \frac{1}{2}\sigma^2\nu\frac{\partial^2 Q_k}{(\partial\nu)^2} + \rho\sigma\nu S(t,\tau_1,\tau_2)\frac{\partial^2 Q_k}{\partial x\partial\nu} = 0\,,\end{aligned} \tag{C.6}$$

for $\alpha_1 = \frac{1}{2}$, $\alpha_2 = -\frac{1}{2}$, $\beta_1(t,\tau_1,\tau_2) = \kappa + \sigma\rho(\xi(t,\tau_1,\tau_2) - S(t,\tau_1,\tau_2))$, and $\beta_2(t,\tau_1,\tau_2) = \kappa + \sigma\rho\xi(t,\tau_1,\tau_2)$. This PDE can be solved by a martingale depending on the solutions of the dynamics

$$dX_k(t) = \alpha_k S^2(t,\tau_1,\tau_2)\nu_k(t)dt + S(t,\tau_1,\tau_2)\sqrt{\nu_k(t)}d\widetilde{W}^F(t)\,,$$
$$d\nu_k(t) = (\kappa\theta(t) - \beta_k(t,\tau_1,\tau_2)\nu_k(t))\,dt + \sigma\sqrt{\nu_k(t)}d\widetilde{W}^\sigma(t)\,.$$

Following Heston, the corresponding characteristic function solves (C.6) as well. Note, that the underlying model structure is of affine type since the PDE is linear in ν. The characteristic function is

thus of exponential affine form (see Duffie (2010)):

$$\hat{Q}_k(t,x,\nu;\phi) = \mathbb{E}_{Q_k}\left[e^{i\phi X_k^{t,x,\nu}(T)}\right] = e^{\Psi_{0k}(t,T,\phi)+\nu\Psi_{1k}(t,T,\phi)+i\phi x}\ , \qquad k=1,2\ , \tag{C.7}$$

for $\phi \in \mathbb{R}$, where $\Psi_{0k}\colon [0,T]\times[0,\tau_1)\times\mathbb{R}\to\mathbb{C}$ and $\Psi_{1k}\colon [0,T]\times[0,\tau_1)\times\mathbb{R}\to\mathbb{C}$ are time-dependent functions satisfying $\Psi_{0k}(T,T,\phi)=0$ and $\Psi_{1k}(T,T,\phi)=0$ at terminal time T. The last term in (C.7) is added in order to ensure the terminal condition

$$\hat{Q}_k(T,x,\nu;\phi) = e^{i\phi x}\ . \tag{C.8}$$

For notational convenience, we drop the time and space indices such that $\Psi_{0k} := \Psi_{0k}(t,T,\phi)$, $\Psi_{1k} := \Psi_{1k}(t,T,\phi)$, and $\hat{Q}_k := \hat{Q}_k(t,x,\nu;\phi)$. Plugging (C.7) into the PDEs of (C.6) for $k=1,2$ and rearranging terms yields

$$\begin{aligned}\hat{Q}_k\Bigg[\nu\Big[\frac{\partial\Psi_{1k}}{\partial t} + \alpha_k S^2(t,\tau_1,\tau_2)i\phi - \Psi_{1k}\beta_k(t,\tau_1,\tau_2) - \frac{1}{2}S^2(t,\tau_1,\tau_2)\phi^2 + \frac{1}{2}\sigma^2\Psi_{1k}^2 \\ + \rho\sigma S(t,\tau_1,\tau_2)i\phi\Psi_{1k}\Big] + \frac{\partial\Psi_{0k}}{\partial t} + \Psi_{1k}\kappa\theta(t)\Bigg] = 0\ .\end{aligned}$$

Since $\hat{Q}_k > 0$ for $k=1,2$ and $\nu>0$ by definition, we apply the *separation of variables argument* (see Duffie (2010); cf. p. 150) to achieve the following differential equations

$$\frac{\partial\Psi_{1k}}{\partial t} = -\frac{1}{2}\sigma^2\Psi_{1k}^2 + \left(\beta_k(t,\tau_1,\tau_2) - \rho\sigma S(t,\tau_1,\tau_2)i\phi\right)\Psi_{1k} + \left(\frac{1}{2}\phi^2 - \alpha_k i\phi\right)S^2(t,\tau_1,\tau_2) \tag{C.9}$$

of Riccati-type and

$$\frac{\partial\Psi_{0k}}{\partial t} = -\Psi_{1k}\kappa\theta(t)\ , \tag{C.10}$$

subject to $\Psi_{0k}(T,T,\phi)=0$ and $\Psi_{1k}(T,T,\phi)=0$ for $k=1,2$.

An application of the Fourier inversion technique (see Gil-Pelaez (1951)) to (C.7) leads to the cumulative distribution functions Q_1 and Q_2 given by

$$Q_k(t,x,\nu;\log(K)) = \frac{1}{2} - \frac{1}{\pi}\int_0^\infty Re\left(\frac{e^{-i\phi\log(K)}\hat{Q}_k(t,x,\nu;\phi)}{i\phi}\right)d\phi\ , \quad k=1,2\ . \tag{C.11}$$

□

D. On the Solutions of the Differential Equations

To show that there exists a unique solution for the Riccati equations $\Psi_{1k}(t, T, \phi)$ for $k = 1, 2$, transfer them to a homogenoeus second order linear differential equation using the substitution $\Psi_{1k}(t, T, \phi) = \frac{z_k'(t,T)}{\frac{1}{2}\sigma^2 \, z_k(t,T)}$ (see, e.g., Poljanin and Zajcev (2018)). Rewrite the resulting differential equation as a system of first order equations in line with Walter (1996)(cf. p. 103f.). Then, Theorem VI (see Walter (1996)) ensures that there exists a unique solution to the differential system and thus to the second order equation since all matrix elements have continuous real and imaginary parts in trading time $t \in [0, \tau_1]$. Finally resubstitution leads to a unique solution to the Riccati-type equation.